Revisiting the origin of satellites in core-level photoemission of transparent conducting oxides: The case of n-doped SnO_{2}

Francesco Borgatti, J. A. Berger, Denis Céolin, Jianqiang Sky Zhou, Joshua J. Kas, Matteo Guzzo, C. F. McConville, Francesco Offi, Giancarlo Panaccione, Anna Regoutz, David J. Payne, Jean-Pascal Rueff, Oliver Bierwagen, Mark E. White, James S. Speck, Matteo Gatti, and Russell G. Egdell

Phys. Rev. B **97**, 155102 — Published 3 April 2018

DOI: 10.1103/PhysRevB.97.155102

Revisiting the origin of satellites in core level photoemission of transparent conducting oxides: the case of n-doped SnO_2

Francesco Borgatti,[1,*] J.A. Berger,[2,3] Denis Céolin,[4] Jianqiang Sky Zhou,[5,3] Joshua J. Kas,[6] Matteo Guzzo,[7] C.F. McConville,[8] Francesco Offi,[9] Giancarlo Panaccione,[10] Anna Regoutz,[11] David J. Payne,[12] Jean-Pascal Rueff,[4,13] Oliver Bierwagen,[14] Mark E. White,[14] James S. Speck,[14] Matteo Gatti,[5,3,4,†] and Russell G. Egdell[11]

[1] *Consiglio Nazionale delle Ricerche – Istituto per lo Studio dei Materiali Nanostrutturati (CNR-ISMN), via P. Gobetti 101, I-40129 Bologna, Italy*
[2] *Laboratoire de Chimie et Physique Quantiques, IRSAMC, CNRS, Université Toulouse III - Paul Sabatier, 31062 Toulouse, France*
[3] *European Theoretical Spectroscopy Facility (ETSF)*
[4] *Synchrotron SOLEIL, L'Orme des Merisiers, Saint-Aubin, BP 48, F-91192 Gif-sur-Yvette, France*
[5] *Laboratoire des Solides Irradiés, École Polytechnique, CNRS, CEA, Université Paris-Saclay, F-91128 Palaiseau, France*
[6] *Department of Physics, University of Washington, Seattle, Washington 98195-1560, USA*
[7] *Institut für Physik und IRIS Adlershof, Humboldt-Universität zu Berlin, D-12489 Berlin, Germany*
[8] *Department of Physics, School of Sciences, RMIT University, Melbourne, Victoria, 3001, Australia*
[9] *Dipartimento di Scienze, Università di Roma Tre, 00146 Rome, Italy*
[10] *Istituto Officina dei Materiali CNR, Laboratorio TASC, S.S. 14 Km 163.5, AREA Science Park, 34149 Basovizza, Trieste, Italy*
[11] *Inorganic Chemistry Laboratory, Department of Chemistry, University of Oxford, South Parks Road, Oxford OX1 3QR, United Kingdom*
[12] *Department of Materials, Imperial College London, Exhibition Road, London SW7 2AZ, UK*
[13] *Sorbonne Universités, UPMC Université Paris 06, CNRS, Laboratoire de Chimie Physique-Matiére et Rayonnement, 75005 Paris, France*
[14] *Materials Department, University of California, Santa Barbara, California 93106, USA*[‡]

(Dated: March 20, 2018)

The longstanding problem of interpretation of satellite structures in core level photoemission spectra of metallic systems with a low density of conduction electrons is addressed using the specific example of Sb-doped SnO_2. Comparison of *ab initio* many-body calculations with experimental hard X-ray photoemission spectra of the Sn 4*d* states shows that strong satellites are produced by coupling of the Sn core hole to the plasma oscillations of the free electrons introduced by doping. Within the same theoretical framework, spectral changes of the valence band spectra are also related to dynamical screening effects. These results demonstrate that, for the interpretation of electron correlation features in the core level photoelectron spectra of such narrow-band materials, going beyond the homogeneous electron gas electron-plasmon coupling model is essential.

Keywords: SnO_2, antimony, charge carrier doping, photoelectron spectroscopy, HAXPES

Transparent conducting oxides (TCOs) such as ZnO, CdO, SnO_2 and In_2O_3, combine optical transparency in the visible region with high electrical conductivity achieved through n-type doping. These features enable a large variety of device applications in optoelectronics and photovoltaics, including their use as transparent electrodes in flat panel displays, organic light-emitting diodes, and solar cells[1–3]. TCOs behave as dilute-electron systems whose density of conduction electrons is much lower than for simple metals, thus offering also an ideal platform to investigate the effects of electronic correlation through the interpretation of the satellite structures occurring in the X-ray photoemission spectra (PES) of core level and valence states. While it was recognized early on that plasmon satellites invariably accompany the main core level peaks in the PES of simple metals[4,5], the interpretation of satellite structures observed for TCOs and other "narrow band" metallic oxides has remained controversial despite the large number of studies[6–14]. After the emission of the photoelectron, as a direct consequence of many-body interactions, the remaining electronic system can be left in different final states giving rise to several lines in the spectrum. Satellites in PES are hence a genuine fingerprint of electronic correlation. In simple metals they were successfully explained on the basis of the homogeneous electron gas (HEG) model as the additional excitation of multiple plasmons[15–18], i.e. quantized charge density oscillations resulting from the long-range nature of the Coulomb interaction. In dilute-electron systems, plasmon energies are typically around 1 eV, which is much smaller than in simple metals and comparable both with the intrinsic core linewidths and with the chemical shifts associated to changes of the oxidation state. Moreover, while in simple metals – as predicted by the HEG model – the overall lineshape involves multiple plasmon loss satellites, for the "narrow band" metals only a single satellite is observed. Therefore, alternative explanations have been put forward, either in terms of mixed valency in the initial state[19], or on the basis of localisation of conduction band

states by the Coulomb potential of the core hole[6,7,20–22].

Solving the ambiguity of the core double-peak structure problem for these systems calls for a joint experimental and theoretical advanced approach. To this end, in the present work we combine hard x-ray photoelectron spectroscopy (HAXPES) with *ab initio* many-body theory to explain the origin of satellites in the core level spectra of the prototypical undoped and Sb-doped SnO_2 TCO. We show that experiments and calculations correlate unambiguously the changes of the valence band (VB) spectrum and the satellite of the core level Sn 4*d* peak to the intrinsic plasma oscillations of the free electrons that are introduced by charge carrier doping. The adoption of HAXPES ensures the sensitivity to the electronic structure of the bulk. Since the intensity of the final-state satellite structure in highly correlated metallic oxides strongly depends on the experimental information depth it is, in some cases, only evident throughout HAXPES.[23–27] The calculations combine the GW approximation (GWA)[28] for the self-energy and the cumulant (C) expansion of the Green's function into the first-principle GW+C scheme[29]. Such an *ab initio* approach, not involving any choice of parameters as in semi-empirical models, establishes which of the conflicting interpretations provided up to now is correct, thus solving definitively the debate that has lasted for decades on the effects of carrier doping on the photoemission spectra of transition metal oxides. Moreover, our results further demonstrate that the GW+C method is accurate, predictive and largely transferable (i.e. not material specific). In fact, this approach has lately been employed in simple metals and semiconductors (including doping effects)[30–40], giving results in very good agreement with experiment. The application of this *ab initio* theory to spectral features of different binding energy (BE) for a typical TCO thus opens the perspective towards the reliable interpretation of electron correlation features in the PES of a large variety of TCO compounds and other conductive oxide materials.

The HAXPES core level spectra in the O 1*s*, Sn $3d_{5/2}$ and Sn 4*d* region of nominally undoped SnO_2 and Sb-doped SnO_2 samples, grown by plasma assisted molecular beam epitaxy, are shown in Fig. 1. The carrier concentration is $3.8\text{x}10^{17}$ cm^{-3} (nominally undoped) and $2.6\text{x}10^{20}$ cm^{-3} (doped sample), respectively[41,42]. The spectra were obtained at the GALAXIES beamline of the SOLEIL synchrotron radiation source using hard X-rays of about $h\nu = 4$ keV and normal emission detection geometry[43,44]. This condition provides an information depth of about 15 nm, large enough to ensure sensitivity to the electronic structure of the bulk and to minimize the contribution of the surface region. All the spectra for the doped sample exhibit a broadening on the high BE side of the peaks that leads them to have an asymmetric profile, with a small shift to higher binding energy of the peak maximum. The fitting analysis of these spectra has been performed consistently with the procedure implemented for previous XPS results.[12] Disentangling the

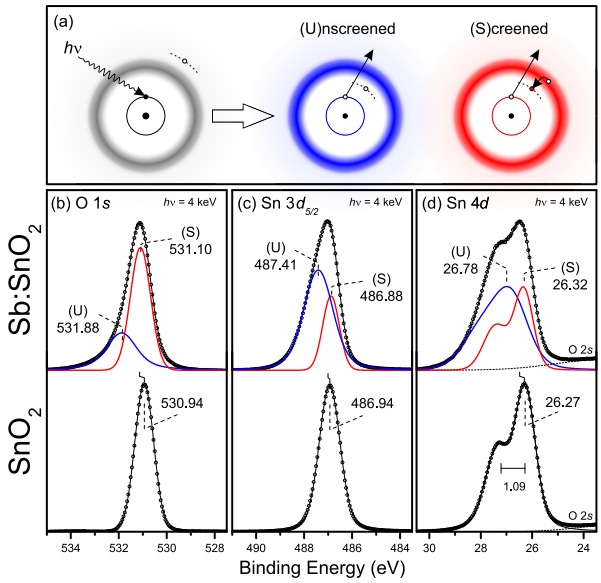

Figure 1. (a) Scheme of the final-state configurations for the (S)creened and (U)nscreened channels accordingly to the Kotani-Toyazawa models[20,22]. (b-d) Core level HAXPES spectra of O 1*s*, Sn $3d_{5/2}$ and Sn 4*d* for nominally undoped SnO_2 (bottom) and Sb-doped SnO_2 (top), respectively. The background of the spectra has been subtracted using a Shirley profile.

spectral terms by Voigt functions in all cases shows a single peak for the undoped sample and two peaks separated by 0.78 eV (O 1*s*) and 0.53 eV (Sn $3d_{5/2}$) for the doped one, while the shallow 4*d* spectrum can be fitted by one or two Voigt pairs with a spin-orbit splitting energy of 1.09 eV and with an additional weak contribution from the O 2*s* level, in agreement with previous XPS results for this and other TCOs[12,14,45]. Further details of the characteristics of the samples, experimental conditions and fit analysis are reported in Ref. 46. In Fig. 1(b-d) we have named the spectral terms for Sb-doped SnO_2 according to the traditional description based on the Kotani-Toyazawa models[20], schematically shown in Fig. 1(a), for which two different final states are accessible depending on whether a localised state pushed below the Fermi level remains empty, giving an "unscreened" state (U), or is filled by transfer of an electron from the conduction band to give a "screened" final state (S)[6,7,20,21]. In these models, the screened final state gives rise to an asymmetric line to low BE side of the lifetime-broadened peak associated with the unscreened final state. We will now show how the *ab initio* theory, that explicitly takes into account the dynamical screening of the photohole, is able to explain these experimental findings without the need to resort to an empirical model approach that requires parameters obtained from experimental data.

The diagonal element of the spectral function for the *i*-th state is the imaginary part of the one-particle Green's function: $A_i(\omega) = \pi^{-1}|\text{Im}G_i(\omega)|$. In the cumulant expansion, merged with the GWA for the self-energy Σ^{xc},

the Green's function G_i (for a hole state of energy smaller than the Fermi level μ) is expressed as

$$G_i(\omega) = \frac{i}{2\pi}\int_{-\infty}^{0} dt e^{i(\omega-\varepsilon_i)t}e^{C_i(t)} \quad (1)$$

$$C_i(t) = \frac{1}{\pi}\int_{-\infty}^{\mu-\varepsilon_i} d\omega \frac{e^{-i\omega t}-1}{\omega^2}\mathrm{Im}\Sigma_i^{xc}(\omega+\varepsilon_i). \quad (2)$$

Here, the quasiparticle (QP) energy ε_i in the energy-self-consistent GW scheme is calculated as: $\varepsilon_i = \varepsilon_i^H + \mathrm{Re}\Sigma_i^{xc}(\varepsilon_i)$, where ε_i^H is the Hartree energy. In the GWA, the self-energy $\Sigma^{xc}(\omega)$ is the convolution of the Green's function $G(\omega)$ and the dynamically screened Coulomb interaction $W(\omega) = \epsilon^{-1}(\omega)v_c$, with v_c being the bare Coulomb interaction that is screened by the inverse dielectric function $\epsilon^{-1}(\omega)$. Since in the GWA $\mathrm{Im}\Sigma^{xc}(\omega)$ is proportional to the loss function $-\mathrm{Im}\epsilon^{-1}(\omega)$, the cumulant $C_i(t)$ describes the *dynamical screening* of the hole ε_i through the coupling with the bosonic charge excitations ω_s, which are the plasmons and many-body interband transitions appearing as peaks in the loss function. Therefore, the first term in Eq. (1) yields the QP peak located at ε_i, while the exponential of $C_i(t)$ in (1) generates satellite structures at multiples of the bosonic energies ω_s away from the QP peak. In the past, the $A_i(\omega)$ of core levels have been extensively obtained using *model* approaches[5,22]. In Ref.[16] Langreth demonstrated that for an isolated core level the cumulant expansion (2) yields the exact solution of the electron-boson model in the specific case of the HEG. On the other hand, Kotani and Toyazawa[20] took into account the screening of the core hole by adopting a single-impurity Anderson model consisting of a localized state and conduction electrons. Instead, in the *ab initio* calculations for SnO_2 we can now make direct use of the band-structure information for the *real* system. Doping is simulated by adding a HEG-type free-carrier contribution in the calculation of $\epsilon^{-1}(\omega)$. To consider the doping dependence, the free-carrier concentration is similar to the experimental value as well as larger by one order of magnitude. All the calculations presented in the following were convoluted by a gaussian function to account for the experimental resolution[46]. We note that the calculated spectra include a lorentzian broadening due to the imaginary part of the self-energy. The convolution of gaussian and lorentzian lineshapes supports the adoption of the Voigt function for the spectral analysis.

The numerical results for the Sn 4*d* core level are shown in Fig. 2 in which the QP contributions have also been singled out[47]. The spin-orbit coupling is not included in the calculations, hence only a single peak is present. Noticeably, in the undoped case (black curves) the full spectral function coincides with the QP-only part: all the structures in the spectrum are hence exclusively due to QP excitations. Upon doping the QP contributions remain the same and only a small shift of about 0.05 eV is found. Doping mostly affects the incoherent part of the spectral function: through a change of the dynamical screening $\epsilon^{-1}(\omega)$, it induces a modification of electronic

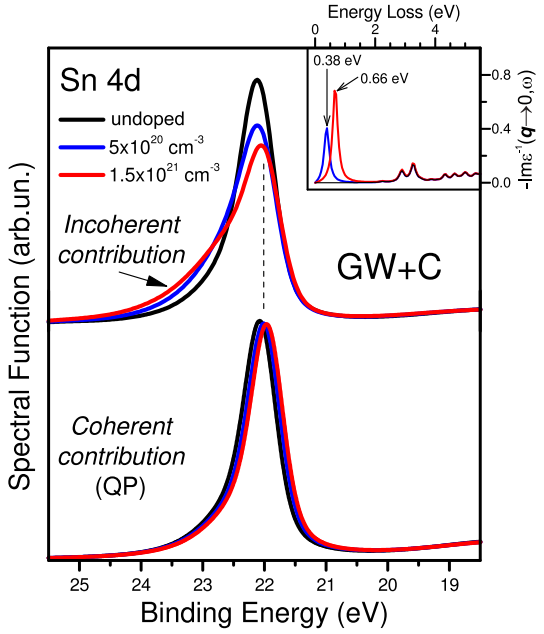

Figure 2. (top) GW+C spectral function for the Sn 4*d* region of undoped (black) and doped (blue, red) compounds, the latter corresponding to two different carrier concentrations. (bottom) quasi-particle (QP) contribution. Inset: Loss function calculated for the same carrier concentrations.

correlations *beyond* the QP picture. Within the GW+C framework this correlation effect can be understood in terms of coupling of core hole and neutral excitations. In order to trace its origin, we have hence also calculated the loss function $-\mathrm{Im}\epsilon^{-1}(\mathbf{q},\omega)$ [inset of Fig. 2 for the $\mathbf{q}\to 0$ limit]. For a finite carrier density we find a new plasmon peak in the loss function at an energy corresponding to the separation between the QP and the new incoherent structures in the spectral function. Conversely, the loss function of a homogenous electron gas with a density equal to the carrier concentration of doped SnO_2 provides a plasmon peak shifted to the much higher energy of about 1.4 eV[46]. Hence we can safely conclude that the broadening of the Sn 4*d* spectrum for the doped SnO_2 is the fingerprint of the correlation effect coupling the 4*d* photoelectrons with the collective oscillation of the free carriers introduced in the material by doping. This mechanism should also be effective for the other core level spectra in Fig. 1, although they cannot be simulated with our pseudopotential approach.

In Fig. 2 we have also investigated what happens in the calculated spectral function when the doping level is changed. According to the expectations based on the weak-coupling limit of the HEG model[16], the intrinsic plasmon satellite intensity for an isolated core level should increase as the conduction electron density n_c decreases[18,48]. At variance with these expectations, the intensity of the satellite decreases and merges with the QP broad structure making it hardly discernible. Moreover, in the *ab initio* calculations at most only one satel-

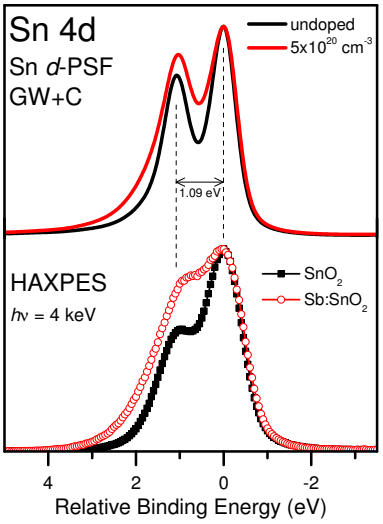

Figure 3. Comparison of HAXPES Sn 4*d* spectra (bottom) and *d*-orbital projection (*d*-PSF) of the spectral functions (top) for undoped and doped SnO_2. All curves are aligned to the position of the experimental Sn $4d_{5/2}$ term.

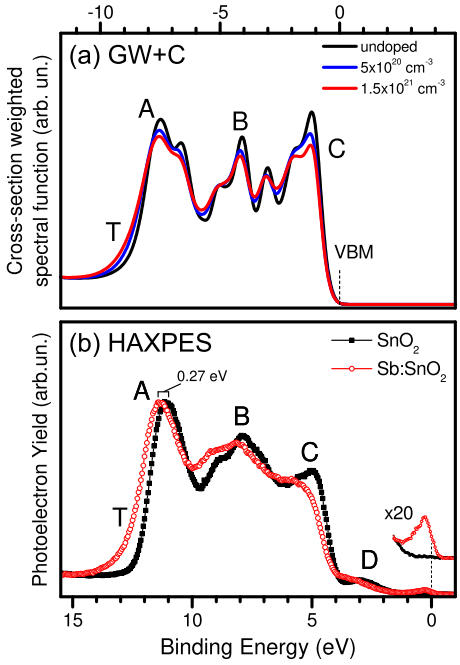

Figure 4. (a) GW+C spectral functions whose angular-projected contributions have been weighted by the respective photoionization cross sections[50]. (b) HAXPES VB spectra normalized to the maximum intensity of the stronger features. The spectral contribution of the conduction states for the doped sample has been enhanced by a factor 20.

lite is clearly visible in the spectra in agreement with HAXPES results, rather than a series of multiple plasmon satellites as predicted by the HEG model. These results therefore show that, in order to capture the satellite structures for narrow-band materials, it is essential to go beyond the HEG electron-plasmon coupling model Hamiltonian[15,16] and to perform *ab initio* calculations that are materials specific.

The support for this conclusion comes through the close matching of theoretical and experimental results. To this aim, in Fig. 3 the Sn 4*d* HAXPES spectra have been aligned to the maximum of the Sn $4d_{5/2}$ peak to manifest more explicitly the broadening on the high BE side of the spectrum for doped SnO_2 after the subtraction of the Shirley background and of the O 2*s* contribution close to the low BE side of the region. The spectra are compared to the *d*-orbital projection of the spectral functions (*d*-PSF) for which the spin-orbit splitting has been phenomenologically included by adding the same curve shifted for the experimental spin-orbit value (1.09 eV) and scaled to achieve the statistical branching ratio of *d*-doublets. Despite the implicit rough approximations of this treatment, the qualitative agreement with experiment is very good, especially considering that extrinsic effects, due to inelastic losses of the outgoing photoelectrons, and their interference with intrinsic contributions, are not included in the calculations[5,49].

Further, in Fig. 4 we consider the valence band (VB) spectra which, for both the pure and the doped compounds, display a three-peaked structure (A-C) in agreement with XPS data previously reported[12]. For the undoped sample, the onset of the valence band maximum (VBM) is placed through linear extrapolation at about 3.84 eV BE relative to the Fermi level E_F, slightly larger than the quoted bulk band gap of 3.62 eV[51]. On the low BE side, the spectra have a weak but well-defined feature (D) that tails into the bulk band gap, which was interpreted as a contribution from lone-pair Sn 5*s*-states occurring at the sample surface and, for the doped sample, concerns also Sb 5*s*-5*p* states[52]. Looking at the position of the stronger features (A), the spectrum of the Sb-doped SnO_2 is shifted to higher BE by 0.27 eV, and the shift of the conduction states below E_F is clearly visible as well as the broadening of the tail (T) on the high BE side. The comparison of the VB states with the calculated spectral function, whose angular-projected contributions have been weighted by the correspondent values of the photoionization cross sections[50], shows that the calculations provide correctly all the relevant features of the experimental VB spectra: (i) the position of the main peaks with respect to the valence band maximum, (ii) the broadening induced by the free-carrier doping, and (iii) the enhancement of the asymmetric tail at the bottom of the valence band. The latter, in particular, confirms Hedin's predictions based on the HEG for valence electrons[53]. In the past, asymmetric tails have often been modeled for core levels using *ad hoc* Doniach-Sunjic or Mahan lineshapes[5,54,55]. In the present case, instead, this result emerges consistently from the same *ab initio* framework that is used for *both* the Sn 4*d* states and the VB. Thus, as for the satellite of the Sn 4*d* core line, this tail can be associated with dynamical screening

effects requiring to go beyond a single-particle picture. This is a direct consequence of the frequency dependence of $\mathrm{Im}\Sigma^{xc}(\omega)$[17,18,53], which is related to the presence of low-energy ($\sim$ 1-2 eV) density fluctuations that couple with high-energy QP excitations in the photoemission spectra[33,56]. On the other hand, the relative intensity of spectral features A-C does not match the experimental results properly, although the slightly larger reduction of B-C vs A with increasing doping is qualitatively reproduced. This mismatch might be partially ascribed, besides the intrinsic correlation effects, to the method adopted to account for the dependence of the photoemission process on the photon energy and polarization, which, in principle, should be included through explicit calculation of the matrix elements within the one-step model of photoemission. This theoretical approach is quite complicated and clearly beyond the scope of this work. However, the weighting of the angular-projected terms by the photoionisation cross-sections improves the agreement with the experiment significantly.[46] These results confirm the reliability of this approach and will surely stimulate further efforts to get a better agreement among the theory and the experiment.

In conclusion, we have elucidated the origin of the satellite structure observed in the Sn 4*d* core level photoemission spectrum of Sb-doped SnO_2 by comparing experimental measurements to results obtained from *ab initio* many-body theory. We have demonstrated that such a satellite is produced by the coupling of the Sn 4*d* core electrons to the plasma oscillation of the free electrons introduced in the material by doping. Moreover, within the same theoretical framework we were able to explain also the enhancement of the asymmetric tail in the valence band photoemission spectrum of doped SnO_2. These results demonstrate that, in order to capture the satellite structures for narrow-band materials and identify properly the underlying electronic structure excitations, it is essential to go beyond the HEG electron-plasmon coupling model and to perform material-specific *ab initio* calculations. In this perspective, the results for the Sb-doped SnO_2 TCO suggest that the GW+C theory can be a very promising approach for the interpretation of electron correlation features in the PES spectra of several conductive oxide materials.

ACKNOWLEDGMENTS

This research was supported by a Marie Curie FP7 Integration Grant within the 7th European Union Framework Programme. Computational time was granted by GENCI (Project No. 544). Support for JJK was provided by DOE BES Grant No. DE-FG02-97ER45623.

* francesco.borgatti@cnr.it
† matteo.gatti@polytechnique.fr
‡ Present address: Paul-Drude-Institut für Festkörperelektronik, 10117 Berlin, Germany

[1] E. Fortunato, D. Ginley, H. Hosono, and D. C. Paine, MRS Bulletin **32**, 242 (2007).
[2] K. Ellmer, Nat Photon **6**, 809 (2012).
[3] J. Gao, K. Kempa, M. Giersig, E. M. Akinoglu, B. Han, and R. Li, Advances in Physics **65**, 553 (2016).
[4] H. Höchst, P. Steiner, and S. Hüfner, Zeitschrift für Phys. B Condens. Matter **30**, 129 (1978).
[5] S. Hüfner, *Photoelectron Spectroscopy: Principles and Applications* (Springer, Berlin, 2003).
[6] M. Campagna, G. K. Wertheim, H. R. Shanks, F. Zumsteg, and E. Banks, Phys. Rev. Lett. **34**, 738 (1975).
[7] J. N. Chazalviel, M. Campagna, G. K. Wertheim, and H. R. Shanks, Phys. Rev. B **16**, 697 (1977).
[8] P. P. Edwards, R. G. Egdell, I. Fragala, J. B. Goodenough, M. R. Harrison, A. F. Orchard, and E. G. Scott, J. Solid State Chem. **54**, 127 (1984).
[9] N. Beatham, P. A. Cox, R. G. Egdell, and A. F. Orchard, Chem. Phys. Lett. **69**, 479 (1980).
[10] P. A. Cox, J. B. Goodenough, P. J. Tavener, D. Telles, and R. G. Egdell, J. Solid State Chem. **62**, 360 (1986).
[11] P. A. Cox, R. G. Egdell, J. B. Goodenough, A. Hamnett, and C. C. Naish, J. Phys. C Solid State Phys. **16**, 6221 (1983).
[12] R. G. Egdell, J. Rebane, T. J. Walker, and D. S. L. Law, Phys. Rev. B **59**, 1792 (1999).
[13] V. Christou, M. Etchells, O. Renault, P. J. Dobson, O. V. Salata, G. Beamson, and R. G. Egdell, J. Appl. Phys. **88**, 5180 (2000).
[14] J. J. Mudd, T.-L. Lee, V. Muñoz-Sanjosé, J. Zúñiga-Pérez, D. Hesp, J. M. Kahk, D. J. Payne, R. G. Egdell, and C. F. McConville, Phys. Rev. B **89**, 035203 (2014).
[15] B. I. Lundqvist, Phys. der Kondens. Mater. **6**, 193 (1967); **6**, 206 (1967).
[16] D. C. Langreth, Phys. Rev. B **1**, 471 (1970).
[17] L. Hedin, B. I. Lundqvist, and S. Lundqvist, J. Res. NBS **74A**, 417 (1970).
[18] L. Hedin, J. Phys. Condens. Matter **11**, R489 (1999).
[19] B. A. De Angelis and M. Schiavello, Chem. Phys. Lett. **38**, 155 (1976); B. A. de Angelis and M. Schiavello, **58**, 249 (1978).
[20] A. Kotani and Y. Toyozawa, J. Phys. Soc. Japan **37**, 912 (1974).
[21] G. K. Wertheim, Chem. Phys. Lett. **65**, 377 (1979).
[22] F. M. F. De Groot and A. Kotani, *Core Level Spectroscopy of Solids*, Advances in Condensed Matter Science (Taylor & Francis Group, 2008).
[23] G. Panaccione, M. Altarelli, A. Fondacaro, A. Georges, S. Huotari, P. Lacovig, A. Lichtenstein, P. Metcalf, G. Monaco, F. Offi, L. Paolasini, A. Poteryaev, O. Tjernberg, and M. Sacchi, Phys. Rev. Lett. **97**, 116401 (2006).
[24] F. Offi, P. Torelli, M. Sacchi, P. Lacovig, A. Fondacaro, G. Paolicelli, S. Huotari, G. Monaco, C. S. Fadley, J. F. Mitchell, G. Stefani, and G. Panaccione, Phys. Rev. B **75**, 014422 (2007).
[25] F. Offi, N. Mannella, T. Pardini, G. Panaccione, A. Fondacaro, P. Torelli, M. W. West, J. F. Mitchell, and C. S.

Fadley, Phys. Rev. B **77**, 174422 (2008).
[26] J. Fujii, M. Sperl, S. Ueda, K. Kobayashi, Y. Yamashita, M. Kobata, P. Torelli, F. Borgatti, M. Utz, C. S. Fadley, A. X. Gray, G. Monaco, C. H. Back, G. van der Laan, and G. Panaccione, Phys. Rev. Lett. **107**, 187203 (2011).
[27] T. Pincelli, V. Lollobrigida, F. Borgatti, A. Regoutz, B. Gobaut, C. Schlueter, T. L. Lee, D. J. Payne, M. Oura, K. Tamasaku, A. Y. Petrov, P. Graziosi, F. M. Granozio, M. Cavallini, G. Vinai, R. Ciprian, C. H. Back, G. Rossi, M. Taguchi, H. Daimon, G. van der Laan, and G. Panaccione, Nature Communications **8**, 16051 (2017).
[28] L. Hedin, Phys. Rev. **139**, A796 (1965).
[29] R. M. Martin, L. Reining, and D. M. Ceperley, *Interacting Electrons: Theory and Computational Approaches* (Cambridge University Press, 2016).
[30] F. Aryasetiawan, L. Hedin, and K. Karlsson, Phys. Rev. Lett. **77**, 2268 (1996).
[31] A. S. Kheifets, V. A. Sashin, M. Vos, E. Weigold, and F. Aryasetiawan, Phys. Rev. B **68**, 233205 (2003).
[32] M. Guzzo, G. Lani, F. Sottile, P. Romaniello, M. Gatti, J. J. Kas, J. J. Rehr, M. G. Silly, F. Sirotti, and L. Reining, Phys. Rev. Lett. **107**, 166401 (2011).
[33] M. Gatti and M. Guzzo, Phys. Rev. B **87**, 155147 (2013).
[34] J. Lischner, D. Vigil-Fowler, and S. G. Louie, Phys. Rev. Lett. **110**, 146801 (2013).
[35] M. Guzzo, J. J. Kas, L. Sponza, C. Giorgetti, F. Sottile, D. Pierucci, M. G. Silly, F. Sirotti, J. J. Rehr, and L. Reining, Phys. Rev. B **89**, 085425 (2014).
[36] J. Lischner, G. K. Pálsson, D. Vigil-Fowler, S. Nemsak, J. Avila, M. C. Asensio, C. S. Fadley, and S. G. Louie, Phys. Rev. B **91**, 205113 (2015).
[37] F. Caruso, H. Lambert, and F. Giustino, Phys. Rev. Lett. **114**, 146404 (2015).
[38] J. S. Zhou, J. J. Kas, L. Sponza, I. Reshetnyak, M. Guzzo, C. Giorgetti, M. Gatti, F. Sottile, J. J. Rehr, and L. Reining, J. Chem. Phys. **143**, 184109 (2015).
[39] F. Caruso and F. Giustino, Phys. Rev. B **94**, 115208 (2016).
[40] C. Verdi, F. Caruso, and F. Giustino, Nature Communications **8**, 15769 (2017).
[41] M. E. White, M. Y. Tsai, F. Wu, and J. S. Speck, Journal of Vacuum Science and Technology A **26**, 1300 (2008).
[42] M. E. White, O. Bierwagen, M. Y. Tsai, and J. S. Speck, Journal of Applied Physics **106**, 093704 (2009).
[43] J.-P. Rueff, J. M. Ablett, D. Ceolin, D. Prieur, T. Moreno, V. Baledent, B. Lassalle-Kaiser, J. E. Rault, M. Simon, and A. Shukla, Journal of Synchrotron Radiation **22**, 175 (2015).
[44] D. Ceolin, J. M. Ablett, D. Prieur, T. Moreno, J. P. Rueff, T. Marchenko, L. Journel, R. Guillemin, B. Pilette, T. Marin, and M. Simon, Journ. El. Spec. Rel. Phen. **190**, 188 (2013).
[45] D. J. Payne, R. G. Egdell, D. S. L. Law, P.-A. Glans, T. Learmonth, K. E. Smith, J. Guo, A. Walsh, and G. W. Watson, J. Mater. Chem. **17**, 267 (2007).
[46] See Supplemental Material [url], which includes Refs. 57–67, for additional results, data analysis, and computational details.
[47] The calculated spectral functions have been aligned to their valence band maximum and not to the Fermi level, as in the experiment, since the work function cannot be determined in calculations for the bulk. Moreover, the binding energy for shallow Sn 4*d* core levels could be improved by QP self-consistency and inclusion of vertex corrections[68–70], however this is not crucial for the present work.
[48] R. G. Egdell, T. J. Walker, and G. Beamson, J. Electron Spectros. Relat. Phenomena **128**, 59 (2003).
[49] L. Hedin, J. Michiels, and J. Inglesfield, Phys. Rev. B **58**, 15565 (1998).
[50] J. H. Scofield, *Theoretical photoionization cross sections from 1 to 1500 keV.* (Lawrence Livermore Lab. Rept. UCRL-51326, 1973).
[51] M. Batzill and U. Diebold, Progress in Surface Science **79**, 47 (2005).
[52] P. A. Cox, R. G. Egdell, C. Harding, W. R. Patterson, and P. J. Tavener, Surface Science **123**, 179 (1982).
[53] L. Hedin, Physica Scripta **21**, 477 (1980).
[54] S. Doniach and M. Sunjic, J. Phys. C **3**, 285 (1970).
[55] G. D. Mahan, Phys. Rev. B **11**, 4814 (1975).
[56] M. Gatti, G. Panaccione, and L. Reining, Phys. Rev. Lett. **114**, 116402 (2015).
[57] S. Tanuma, C. J. Powell, and D. R. Penn, Surf. Interf. Anal. **21**, 165 (1994).
[58] L. Kleinman and D. M. Bylander, Phys. Rev. Lett. **48**, 1425 (1982).
[59] N. Troullier and J. L. Martins, Phys. Rev. B **43**, 1993 (1991).
[60] X. Gonze, Zeitschrift für Krist. - Cryst. Mater. **220**, 558 (2005).
[61] J. Lindhard, Kgl. Danske Vidensk. Selsk. Mat.-Fys, Medd. **28**, 8 (1954).
[62] A. Marini, G. Onida, and R. Del Sole, Phys. Rev. B **64**, 195125 (2001).
[63] H. J. Monkhorst and J. D. Pack, Phys. Rev. B **13**, 5188 (1976).
[64] A. Schleife, J. B. Varley, F. Fuchs, C. Rödl, F. Bechstedt, P. Rinke, A. Janotti, and C. G. Van de Walle, Phys. Rev. B **83**, 035116 (2011).
[65] J. A. Berger, L. Reining, and F. Sottile, Phys. Rev. B **85**, 085126 (2012).
[66] J. J. Kas, J. J. Rehr, and L. Reining, Phys. Rev. B **90**, 085112 (2014).
[67] J. S. Zhou *et al.*, in preparation.
[68] M. van Schilfgaarde, T. Kotani, and S. Faleev, Phys. Rev. Lett. **96**, 226402 (2006).
[69] F. Bruneval and M. Gatti, Top. Curr. Chem. **347**, 99 (2014).
[70] A. Grüneis, G. Kresse, Y. Hinuma, and F. Oba, Phys. Rev. Lett. **112**, 096401 (2014).